

Intrinsic and extrinsic origins of low-frequency noise in GaAs/AlGaAs Schottky-gated nanostructures

Kenichi Hitachi,¹ Takeshi Ota,¹ and Koji Muraki¹

¹*NTT Basic Research Laboratories, NTT Corporation,*

Atsugi-shi, Kanagawa 243-0198, Japan

(Dated: January 16, 2020)

Abstract

We study low-frequency noise in current passing through quantum point contacts fabricated from several GaAs/AlGaAs heterostructures with different layer structures and fabrication processes. In contrast to previous reports, there is no gate-dependent random telegraph noise (RTN) originating from tunneling through a Schottky barrier in devices fabricated using the standard low-damage process. Gate-dependent RTN appears only in devices fabricated with a high-damage process that induces charge trap sites. We show that the insertion of AlAs/GaAs superlattices in the AlGaAs barrier helps to suppress trap formation. Our results enable the fabrication of damage-resistant and thus low-noise devices.

PACS numbers:

Low-frequency noise in the source-drain resistance of metal-oxide-semiconductor and GaAs high-electron-mobility transistors arising from background charge fluctuations have been a long-standing issue [1-3]. As the device size decreases, device properties become increasingly susceptible to local charge fluctuations. The noise can exhibit either $1/f$ or random telegraphic behavior depending on the number of charge trap sites involved [4]. In mesoscopic or nanoscale devices such as quantum point contacts (QPCs) and quantum dots (QDs), single electron hopping occurring at somewhat distant sites can be resolved as a measurable change in the device characteristics. Because of their high charge sensitivity, QPCs have been widely used as charge sensors for detecting individual charges in QDs, which constitutes a key element of the present quantum information technology based on QDs. However, the precision of the state readout is limited by the conductance fluctuation of the QPC arising from uncontrolled background charge motion. Background charge noise also causes fluctuations of the energy levels in QDs, which results in decoherence and gate error in both charge [5-7] and spin qubits [8-10].

Several mechanisms have been considered as the origin of the low-frequency noise in GaAs-based devices, including electron hopping between the two-dimensional electron gas (2DEG) and trap sites [11, 12], current leakage through the Schottky barrier [13-16], and electron hopping within the remote-doping layer [17, 18]. An important observation in these studies is that the low-frequency charge noise increases as the voltage V_g applied to the surface Schottky gate is decreased and becomes more negative. Since the Schottky barrier becomes less opaque with decreasing V_g , the observed V_g dependence was interpreted as evidence that the current leakage through the Schottky barrier was responsible for the charge noise. The strong V_g dependence of the noise, in turn, allowed the reduction of the charge noise by employing bias cooling [14] or an additional global top gate [15], both of which shift the operation point to a less negative voltage. In an attempt to eliminate the charge noise associated with doping, single-electron transistors based on undoped structures have been

fabricated [19]; however, the anticipated noise reduction has not yet been demonstrated.

In this paper, we study the effects of the layer structure and fabrication process on the low-frequency current noise in QPC devices fabricated from GaAs/Al_{0.3}Ga_{0.7}As modulation-doped heterostructures at 4.2 K to clarify the origin of the noise. Specifically, in addition to the standard delta-doped structure, we examined a structure in which AlAs/GaAs superlattice (SL) barriers are inserted above and below the delta-doping layer—if the current leakage through the Schottky barrier is the prime contributor to the charge noise, the noise should be suppressed by employing the SL barriers, as suggested in Ref. 15. As opposed to previous reports [14, 15] and the above expectation, we found the noise in our devices to be nearly V_g independent and unaffected by the SL barriers. On the other hand, devices fabricated using a high-damage process that induces charge trap sites exhibited strongly V_g -dependent noise characterized by random telegraphic behavior. We show that the inclusion of SL barriers helps to suppress the formation of trap sites and, accordingly, reduce the process-induced V_g -dependent noise. Our results pave the way to obtaining stable gated nanostructures without bias cooling or a global top gate and assist in the fabrication of damage-resistant devices.

We examined the use of devices with QPC and double quantum dot (DQD) gate layouts, as shown in Fig. 1(a) and (b), respectively, to measure the charge noise. A QPC device is defined by applying the same gate voltage V_g to the center gate C and one of the finger gates Q_i ($i = 1-4$). The gap between C and Q_i ranges from $W = 190$ to 280 nm (in 30-nm steps), which allows the in-situ comparison of QPCs with different operation gate voltages. For the DQD-type devices, a QPC was formed by applying the same V_g to two of eight gates, where the operation voltage was varied by activating a different gate pair. We examined three kinds of layer structures with conduction band profiles as schematically shown in Fig. 1(c)-(e). Type-I is a standard delta-doped structure [Fig. 1(c)]. In type-II, 10-nm-thick AlAs/GaAs (2.1 nm/0.56 nm) SL barriers are inserted above and below the delta-doping

layer [Fig. 1(d)]. A uniform-doped structure (type-III) was also examined [Fig. 1(e)].

The samples we investigated and the wafers we used are listed in Table I together with their properties. In addition to the standard process that we use to fabricate QPC and DQD devices, we also examined the effects of a high-damage process by additionally employing intense UV ozone cleaning at 100 °C for 3 minutes prior to the electron-beam lithography. While this eliminates the remaining photoresist and facilitates the lift-off process, it also induces considerable damage, as evidenced by the decrease in the carrier density and the mobility (sample E, Table I). For the structure with the SL barriers, the same process had much less effect on the carrier density and the mobility (sample F, Table I), which we discuss later. All measurements were performed at 4.2 K. Unless otherwise noted, the results presented below were obtained from devices fabricated with the standard process.

Figure 2(a) shows a typical measurement for sample A. We applied a source-drain voltage of 300 μV and measured the current $I(t)$ through the QPC over 20 seconds at several V_g values with the QPC conductance G_{QPC} below the first plateau, i.e., $0 < G_{\text{QPC}} < 2e^2/h$, where e is an elementary charge and h is Planck's constant. Following the method in Ref. [20], we characterize the charge noise in terms of the equivalent gate voltage noise defined as $\Delta V_g = \Delta I / (d\bar{I}/dV_g)$, where \bar{I} and ΔI are the time average and fluctuation of $I(t)$. Here, ΔI [Fig. 2(d)] was calculated as

$$\Delta I = \sqrt{2 \int_{0.1}^{25} S_I(f) df}$$

using the Fourier power spectrum $S_I(f)$ of $I(t)$, and \bar{I} and $d\bar{I}/dV_g$ [Fig. 2(b) and (c)] were calculated numerically from the data [21]. As shown in Fig. 2(d), ΔI clearly depends on $d\bar{I}/dV_g$, which precludes the noise from the current amplifier as the origin of the observed noise. We note that the voltage noise on the gates is also negligible, as the resolution (3 μV) of the voltage sources that we employed is about one order of magnitude smaller than the measured ΔV_g [Fig. 2(e)]. As shown in Fig. 2(e), ΔV_g is not greatly influenced by a change

in $d\bar{I}/dV_g$ with V_g , and remains nearly constant over the range $0 < G_{\text{QPC}} < 2e^2/h$.

Figure 3 shows ΔV_g measured for QPCs fabricated from four different wafers as a function of operating point V_g . Each data point corresponds to a different gate combination, representing an average taken over several V_g values near the corresponding central operation voltage. The error bars indicate the standard deviation. We first note that, in the standard delta-doped structure (type-I), the measured noise is only weakly dependent on V_g . This also indicates that the measured noise level appropriately reflects the property of the sample and does not depend on the position or specific configuration of the QPC. Such V_g -independent noise is in sharp contrast to that described in Ref. 15, where ΔV_g increased exponentially as V_g was decreased below -0.5 V. As demonstrated in Refs. 14 and 15, ΔV_g increases because decreasing V_g makes the Schottky barrier less opaque and thus enhances the tunneling probability from the gate to the trap sites in the AlGaAs barrier. The absence of such strong V_g dependence in our devices suggests that tunneling through the Schottky barrier is irrelevant to the observed noise. This conjecture is also supported by a comparison of the noise levels of our devices and those studied in Ref. 15. Whereas at a small negative V_g the noise levels in samples A and B are twice that reported in Ref. 15, due to the absence of V_g dependence, these devices exhibit much less noise at a large negative V_g . This enables us to define stable nanostructures such as a QPC or a QD without employing bias cooling or an additional global gate; this is a strong advantage, because it lifts the restrictions on the operation voltage set by bias cooling or a global gate, thereby greatly enhancing the degree of freedom in tailoring desired nanostructures.

As shown in Fig. 3, the insertion of the SL barriers did not reduce the noise level in our devices (type-II). The independence of the charge noise as regards the presence or absence of the SL barriers lends support to the above conjecture that tunneling through the Schottky barrier is irrelevant to the noise observed in our devices. The behavior of the sample fabricated from the uniform-doped structure (type-III) is similar to that of the other samples.

Another important feature of our data is that it is free from random telegraphic, or switching behavior, even for large negative V_g values, as seen in Fig. 2(a). Indeed, we observed no switching noise, or random telegraphic noise (RTN) for measurements obtained over a number of hours. This was true for all the devices that we examined that were fabricated with the standard process, independent of the type of layer structure or doping. Note that RTN appears when only a few trap sites located near the QPC are the prime contributors to the charge fluctuation. The absence of RTN in our devices, combined with the low noise level at a large negative V_g , implies that in our devices there is no trap site available for tunneling electrons near the QPC. This also suggests that switching noise due to tunneling through a Schottky barrier is not necessarily inherent to GaAs-based modulation-doped structures.

The absence of RTN in our devices in turn suggests the existence of extrinsic origins of RTN. To explore this possibility, we examined the effects of process-induced charge traps by additionally employing intense UV ozone cleaning prior to the electron-beam lithography. This process induces charge trap sites, as evidenced by the significant decrease in the mobility (sample E, Table I). As shown in the inset to Fig. 4(a), we did observe RTN in the device fabricated with the intense UV cleaning. In Fig. 4(a), we plot ΔV_g of this device as a function of V_g and compare it with the results obtained for a device fabricated from the same wafer using the standard process. The intense UV cleaning induced strongly V_g -dependent noise that increased rapidly below -0.5 V, which confirms the link between strong V_g dependence and random telegraphic behavior.

Interestingly, we found that the SL barriers played an unexpected role that would allow us to make devices much more resistant to damage from processing. As shown in Table I, the inclusion of SL barriers (sample F) attenuates the deleterious effect that processing has on carrier density and mobility. This is particularly clear for the mobility, which differs by almost one order of magnitude. This result clearly shows that the SL barriers help

to suppress the formation of trap sites. The reduced trap density is also evident in the noise behavior. In contrast to the results for the samples without SL barriers, ΔV_g is barely affected by the high-damage process and remains almost V_g independent as shown in Fig. 4(b). It is possible that the SL barriers block tunneling through the Schottky barrier and thereby suppress the V_g -dependent RTN. In the present case, however, it is more likely that the reduced RTN is due to the lower trap density, as clearly demonstrated by the electron density and the mobility (Table I). Although the exact mechanism for the suppressed trap formation is unknown, our finding enables the fabrication of damage-resistant and thus low-noise devices.

Finally, we discuss the origin of the V_g -independent noise observed in the samples fabricated with the standard low-damage process. In the samples fabricated with the high-damage process, the spatial range over which the trap sites relevant to the RTN are distributed can be crudely estimated from the size of the current step at each switching event. In our DQD-type devices, the operating voltage of the QPC charge sensor shifts by 1.3 (0.9) mV (data not shown) when one electron is added to or removed from the QD on the near (far) side about 300 (400) nm from the QPC. Since the observed RTN corresponds to a shift in the QPC operating voltage a few times larger than these values, we can estimate that the relevant trap sites are distributed within ~ 100 nm of the QPC. This estimate, which also implies that the relevant trap sites are located close to the split gate, is consistent with the noise being strongly V_g dependent. In turn, it follows that the V_g -independent noise dominant in our devices fabricated with the standard process is due to charge hopping taking place at distant sites distributed over a much wider spatial range. This picture is consistent with the absence of switching behavior and V_g dependence. As we discussed above, vertical tunneling through the AlGaAs (or SL) barrier is unlikely to be its origin. We therefore speculate that charge hopping within the remote-doping layer is the most likely cause of the V_g -independent noise. However, we do not know why the noise level differs among wafers

with the identical doping (compare samples A, B, and C in Fig. 3, which all have the same doping level). Indeed, even though device E has high charge trap density, it shows lower noise than sample F at $V_g = -0.4$ V, where RTN is absent (Fig. 4). This result may be attributed to the difference in the starting material. If so, it implies that these process-induced traps do not contribute to the V_g -independent noise. A further investigation is necessary to clarify the origin of the V_g -independent noise.

In summary, we identified two types of low-frequency noise in GaAs/AlGaAs QPCs distinguished by V_g dependence linked with the presence/absence of switching behavior. Our results indicate that the commonly observed V_g -dependent switching noise is not necessarily an intrinsic property of modulation-doped GaAs/AlGaAs heterostructures and point to the importance of eliminating extrinsic origins of low-frequency noise. We found that the inclusion of SL barriers attenuates damage from processing that can be a source of low-frequency noise. Our findings will thus enhance the degree of freedom in tailoring low-noise Schottky-gated nanostructures and assist in the fabrication of devices that are resistant to damage from processing.

Part of this work was supported financially by the MEXT Grant-in-Aid for Scientific Research on Innovative Areas (21102003), and the Funding Program for World-Leading Innovative R&D on Science and Technology (FIRST).

- [1] M. J. Kirton and M. J. Uren, *Advances in Physics*, **38**, 367 (1989).
- [2] Y. P. Li, D. C. Tsui, J. J. Heremans, and J. A. Simmons, *Appl. Phys. Lett.* **57**, 774 (1990).
- [3] D. H. Cobden, N. K. Patel, M. Pepper, D. A. Ritchie, J. E. F. Frost, and G. A. C. Jones, *Phys. Rev. B* **44**, 1938 (1991).
- [4] S. Machlup, *J. Appl. Phys.* **25**, 341 (1954).
- [5] T. Hayashi, T. Fujisawa, H. D. Cheong, Y. H. Jeong, and Y. Hirayama, *Phys. Rev.*

Lett. **91**, 226804 (2003).

[6] K. D. Petersson, J. R. Petta, H. Liu, and A. C. Gossard, Phys. Rev. Lett. **105**, 246804 (2010).

[7] T. Itakura and Y. Tokura, Phys. Rev. B **67**, 195320 (2003).

[8] J. R. Petta, A. C. Johnson, J. M. Taylor, E. A. Laird, A. Yacoby, M. D. Lukin, C. M. Marcus, M. P. Hanson, and A. C. Gossard, Science **309**, 2180 (2005).

[9] Q. Li, L. Cywinski, D. Culcer, X. Hu, and S. Das Sarma, Phys. Rev. B **81**, 085313 (2010).

[10] D. Culcer, X. Hu, and S. Das Sarma, Appl. Phys. Lett. **95**, 073102 (2009).

[11] C. Dekker, A. J. Scholten, F. Liefvink, R. Eppenga, H. van Houten, and C. T. Foxon, Phys. Rev. Lett. **66**, 2148 (1991).

[12] T. Sakamoto, Y. Nakamura, and K. Nakamura, Appl. Phys. Lett. **67**, 2220 (1995).

[13] D. H. Cobden, A. Savchenko, M. Pepper, N. K. Patel, D. A. Ritchie, J. E. F. Frost, and G. A. C. Jones, Phys. Rev. Lett. **69**, 502 (1992).

[14] M. Pioro-Ladriere, J. H. Davies, A. R. Long, A. S. Sachrajda, L. Gaudreau, P. Zawadzki, J. Lapointe, J. Gupta, Z. Wasilewski, and S. Studenikin, Phys. Rev. B **72**, 115331 (2005).

[15] C. Buizert, F. H. L. Koppens, M. Pioro-Ladriere, H-P. Tranitz, I. T. Vink, S. Tarucha, W. Wegscheider, and L. M. K. Vandersypen, Phys. Rev. Lett. **101**, 226603 (2008).

[16] Y. X. Liang, Q. Dong, M. C. Cheng, U. Gennser, A. Cavanna, and Y. Jin, Appl. Phys. Lett. **99**, 113505 (2011).

[17] G. Timp, R. E. Behringer, and J. E. Cunningham, Phys. Rev. B **42**, 9259 (1990).

[18] C. Kurdak, C. J. Chen, D. C. Tsui, S. Parihar, S. Lyon, and G. W. Weimann, Phys. Rev. B **56**, 9813 (1997).

[19] A. M. See, O. Klochan, A. R. Hamilton, A. P. Micolich, M. Aagesen, and P. E. Lindelof, Appl. Phys. Lett. **96**, 112104 (2010).

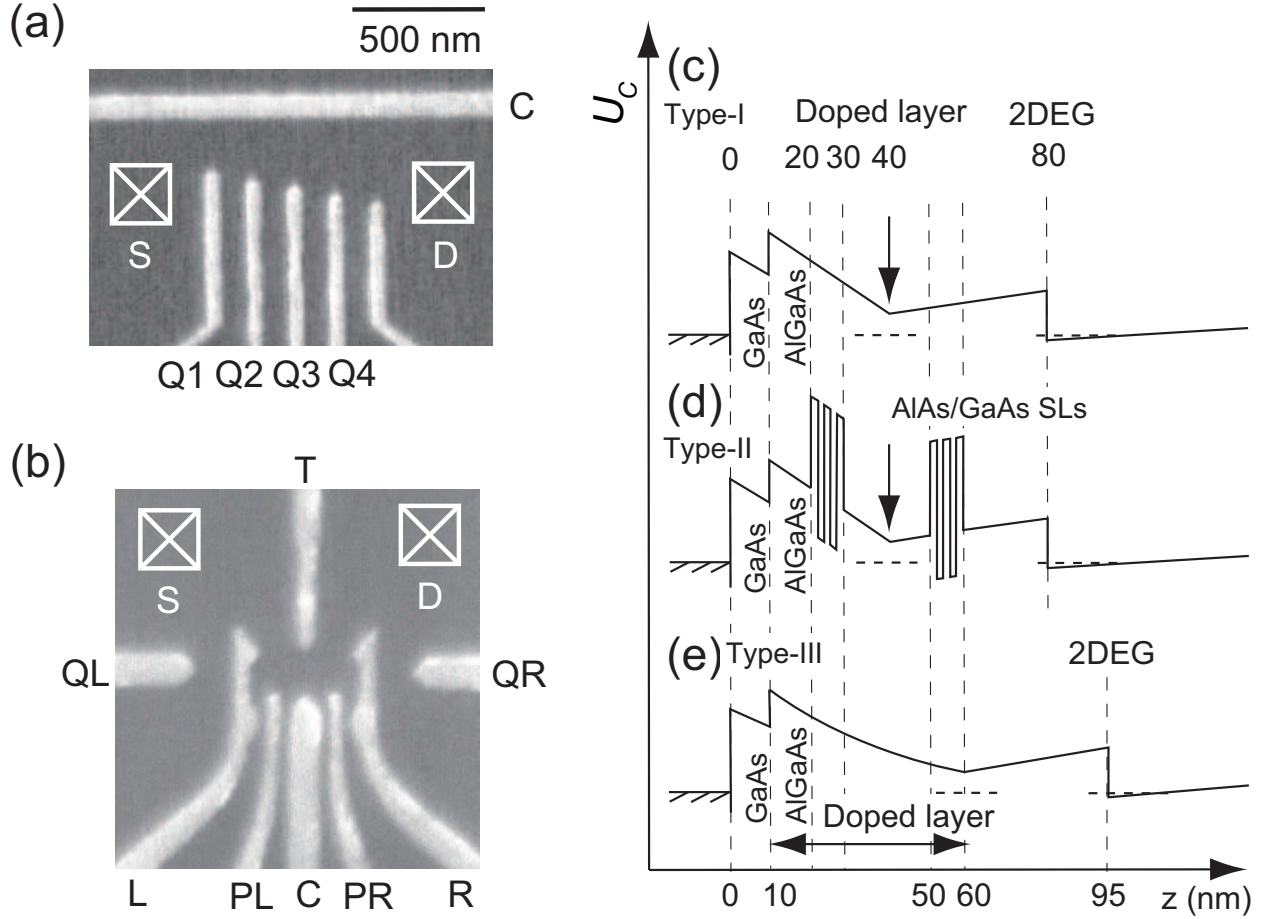


FIG. 1: (Color online) (a), (b) SEM images showing the gate layouts for (a) QPC and (b) DQD devices. (c)-(e) Schematic illustrations of conduction band profiles for (c) a standard delta-doped structure (type-I), (d) a delta-doped structure with AlAs/GaAs SL barriers (type-II), and (e) an uniform-doped structure (type-III). The Si doping density is $4 \times 10^{12} \text{ cm}^{-2}$ for delta doping and $1 \times 10^{18} \text{ cm}^{-3}$ for uniform doping.

[20] S. W. Jung, T. Fujisawa, Y. Hirayama, and Y. H. Jeong, *Appl. Phys. Lett.* **85**, 768 (2004).

[21] We have confirmed that the high-frequency components above 25 Hz have a negligible contribution to ΔI .

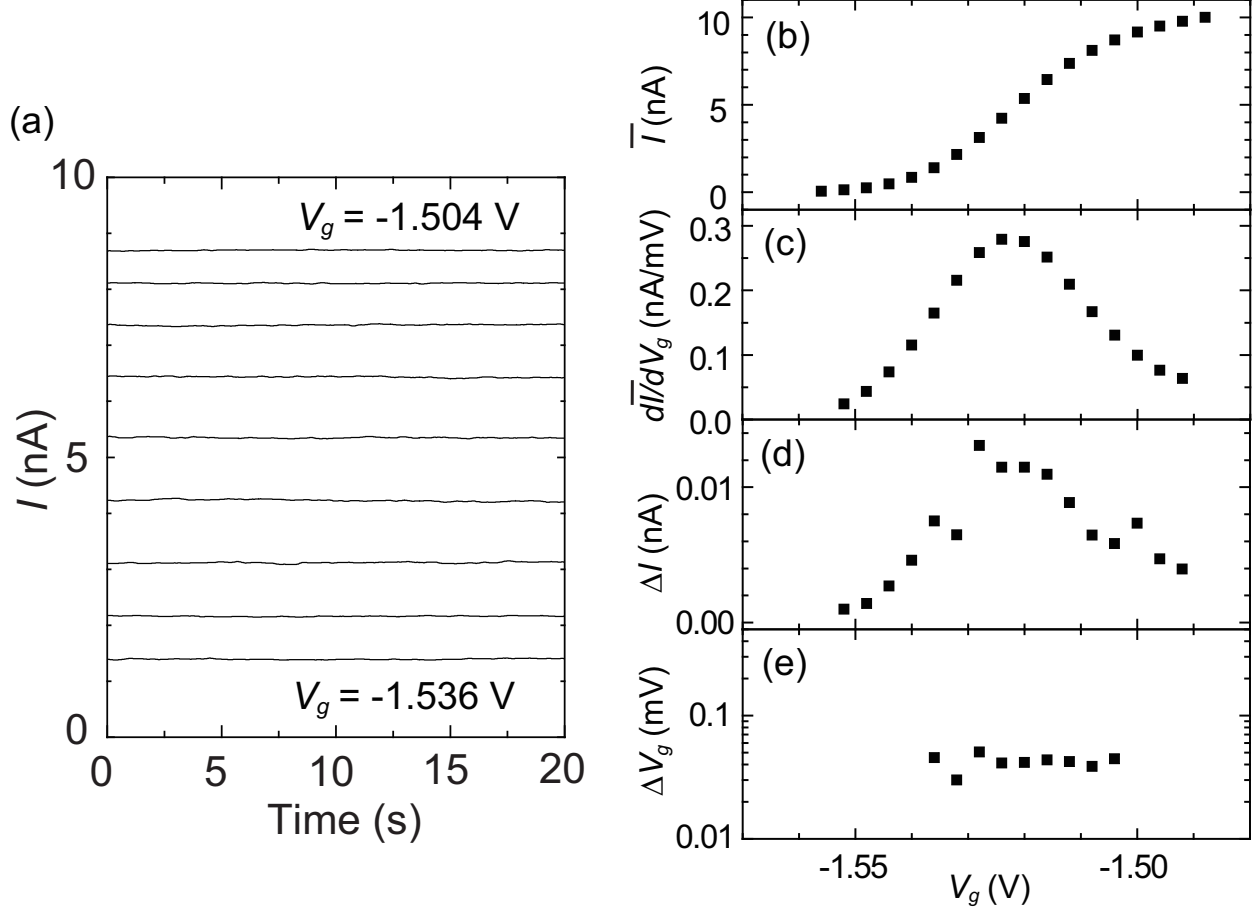


FIG. 2: (Color online) (a) Time traces of current $I(t)$ through the QPC in sample A (type-I) for several V_g values. (b)-(e) Analysis of the time traces $I(t)$ shown in (a): (b) average current \bar{I} , (c) transconductance $d\bar{I}/dV_g$, (d) current fluctuation ΔI , and (e) equivalent gate voltage noise ΔV_g , plotted as a function of V_g .

TABLE I: List of samples and wafers used. The carrier density n and the mobility μ are shown in units of 10^{11} cm^{-2} and $10^6 \text{ cm}^2/\text{Vs}$, respectively.

sample	wafer #	wafer structure	fabrication process	n	μ	gate layout
A	R193	type-I	standard	2.3	1.8	DQD
B	R244	type-I	standard	2.2	1.3	QPC
C	R219	type-II	standard	2.3	1.3	DQD
D	R247	type-III	standard	2.5	2.9	QPC
E	R244	type-I	high-damage	1.9	0.14	QPC
F	R219	type-II	high-damage	2.3	1.2	DQD

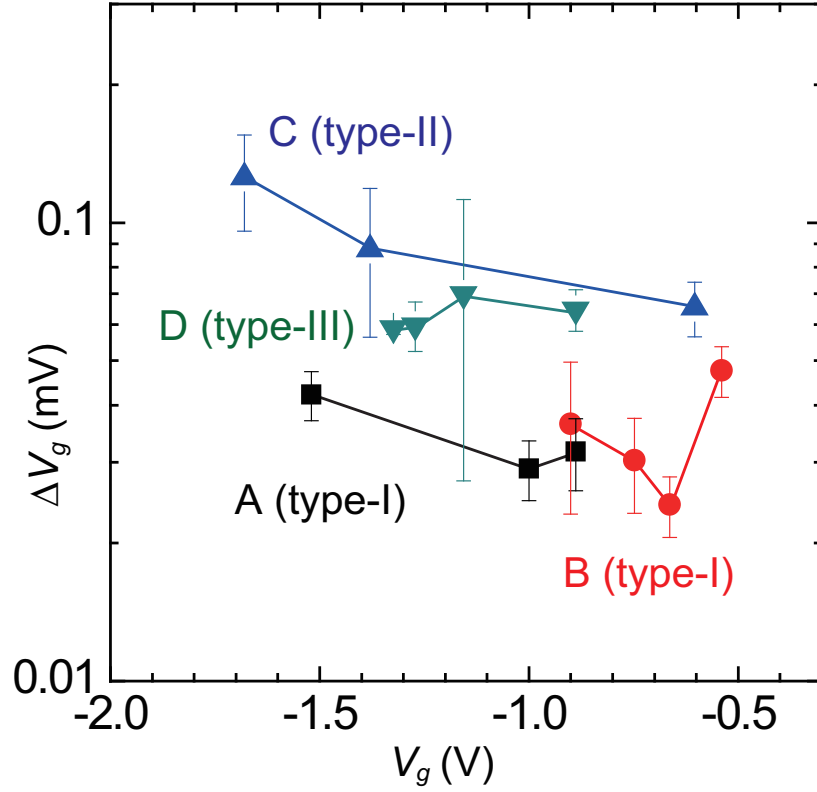


FIG. 3: (Color online) Equivalent gate voltage noise ΔV_g as a function of V_g for samples A to D fabricated from different wafers with various layer structures and doping schemes (see Table I).

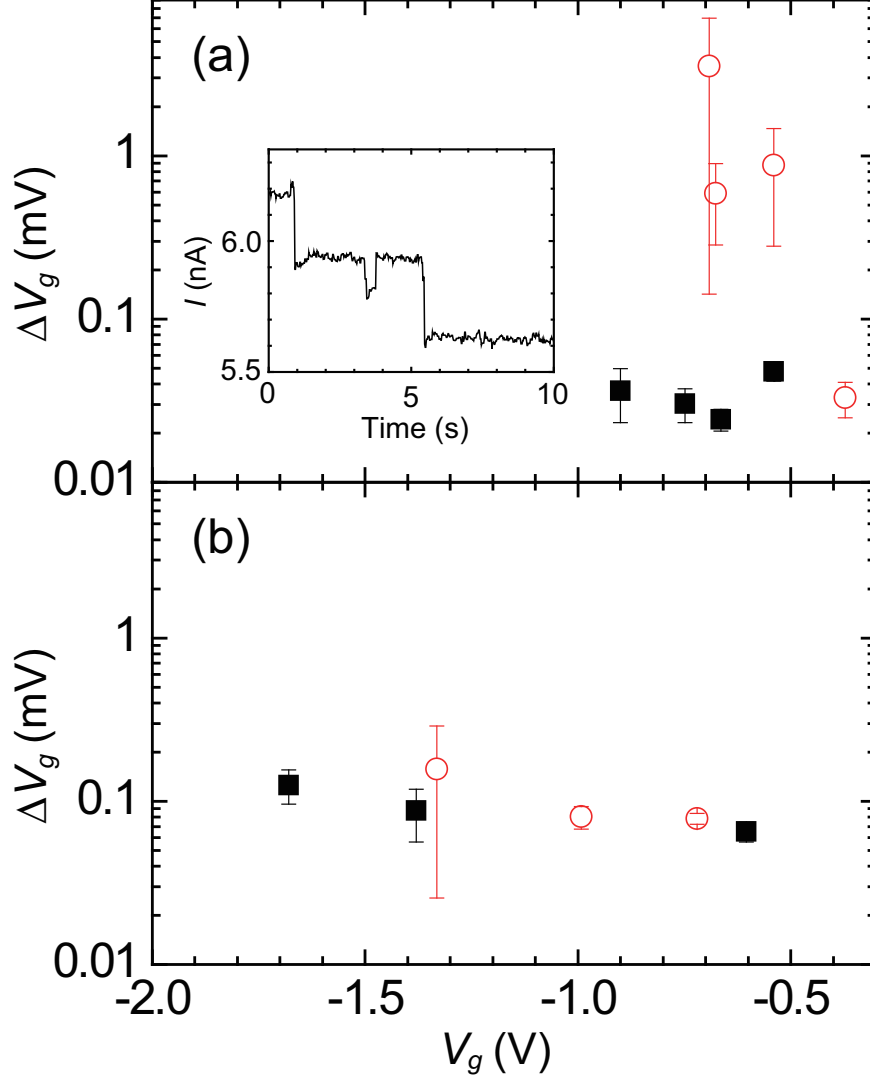


FIG. 4: (Color online) Comparison of equivalent gate voltage noise ΔV_g in samples fabricated from the same wafer using the standard process (solid squares) and with additional intense UV cleaning (open circles): (a) standard delta-doped structure (type-I: samples B and E) and (b) delta-doped structure with SL barriers (type-II: samples C and F). Inset to (a): typical time trace of QPC current in a sample fabricated with intense UV cleaning (sample E).